ISPRS Journal of Photogrammetry and Remote Sensing 137 (2018) 163–174

Contents lists available at ScienceDirect

ISPRS Journal of Photogrammetry and Remote Sensing

journal homepage: www.elsevier.com/locate/isprsjprs

Important LiDAR metrics for discriminating forest tree species in Central Europe

Yifang Shi [a,*], Tiejun Wang [a], Andrew K. Skidmore [a,c], Marco Heurich [b]

[a] Faculty of Geo-Information Science and Earth Observation (ITC), University of Twente, Hengelosestraat 99, P.O. Box 217, 7500 AE Enschede, The Netherlands
[b] Department of Nature Protection and Research, Bavarian Forest National Park, Freyunger Str. 2, 94481 Grafenau, Germany
[c] Department of Environmental Science, Macquarie University, NSW 2109, Australia

ARTICLE INFO

Article history:
Received 30 June 2017
Received in revised form 30 January 2018
Accepted 2 February 2018
Available online 7 February 2018

Keywords:
Tree species
Natural forest
Airborne LiDAR
Morphology
Leaf-on
Leaf-off

ABSTRACT

Numerous airborne LiDAR-derived metrics have been proposed for classifying tree species. Yet an in-depth ecological and biological understanding of the significance of these metrics for tree species mapping remains largely unexplored. In this paper, we evaluated the performance of 37 frequently used LiDAR metrics derived under leaf-on and leaf-off conditions, respectively, for discriminating six different tree species in a natural forest in Germany. We firstly assessed the correlation between these metrics. Then we applied a Random Forest algorithm to classify the tree species and evaluated the importance of the LiDAR metrics. Finally, we identified the most important LiDAR metrics and tested their robustness and transferability. Our results indicated that about 60% of LiDAR metrics were highly correlated to each other ($|r| > 0.7$). There was no statistically significant difference in tree species mapping accuracy between the use of leaf-on and leaf-off LiDAR metrics. However, combining leaf-on and leaf-off LiDAR metrics significantly increased the overall accuracy from 58.2% (leaf-on) and 62.0% (leaf-off) to 66.5% as well as the kappa coefficient from 0.47 (leaf-on) and 0.51 (leaf-off) to 0.58. Radiometric features, especially intensity related metrics, provided more consistent and significant contributions than geometric features for tree species discrimination. Specifically, the mean intensity of first-or-single returns as well as the mean value of echo width were identified as the most robust LiDAR metrics for tree species discrimination. These results indicate that metrics derived from airborne LiDAR data, especially radiometric metrics, can aid in discriminating tree species in a mixed temperate forest, and represent candidate metrics for tree species classification and monitoring in Central Europe.

1. Introduction

Discrimination of tree species is a major task undertaken in a wide range of environmental applications, such as biodiversity monitoring (Shang and Chazette, 2014; Suratman, 2012), ecosystem services assessment (Jones et al., 2010; Skidmore et al., 2015), invasive species detection and control (Boschetti et al., 2007), as well as sustainable forest management (Pcorona et al., 2006). Remote sensing can provide a valuable information source towards our understanding of ecosystem structure and function over large spatial scales (Baldeck et al., 2015). The identification and mapping of tree species is usually conducted through visual interpretation of aerial photographs by human experts coupled with forest inventory (*in situ*) plots, which is labour-intensive, time consuming and costly. More importantly, this method is not practical or applicable to large forested areas (Kim et al., 2009). Optical remote sensing such as airborne or spaceborne multispectral and hyperspectral images have been used to map tree species over the last few decades (e.g. Aspinall, 2002; Boschetti et al., 2007; Feret and Asner, 2013; Immitzer et al., 2012; Jones et al., 2010; Leckie et al., 2003, 2005; Somers and Asner, 2014). However, during the process of developing these remote sensing solutions, it has also been realized that multi- and hyper-spectral images have their own limitations (Heinzel and Koch, 2012). For instance, the same tree species can have different spectral signatures in different parts of forest (Immitzer et al., 2012). Also, different tree species may possess similar spectra as well, particularly in a mixed pixel (Ghiyamat and Shafri, 2010). Furthermore, multi- and hyper-spectral images are generally restricted to the horizontal plane,

* Corresponding author.
E-mail addresses: y.shi-1@utwente.nl (Y. Shi), t.wang@utwente.nl (T. Wang), a.k.skidmore@utwente.nl (A.K. Skidmore), marco.heurich@npv-bw.bayern.de (M. Heurich).

https://doi.org/10.1016/j.isprsjprs.2018.02.002
0924-2716/

providing limited insight pertaining to the vertical profile of tree structure (Jones et al., 2010).

Recent developments in active remote sensing, particularly the light detection and ranging (LiDAR) technique, have shown great potential for tree species mapping due to its capability of capturing three-dimensional (3D) information of objects of interest (Brandtberg, 2007; Clark et al., 2004; Coops et al., 2007; Holmgren and Persson, 2004; Hyyppä et al., 2001; Lindberg et al., 2014; Næsset, 2002). Unlike multi- and hyper-spectral images, it is possible to retrieve structural properties of trees from LiDAR, based on the discrete points or full-waveform data (Alonzo et al., 2014; Asner et al., 2008; Coops et al., 2007; Dalponte et al., 2014; Onojeghuo and Blackburn, 2011; Shang and Chazette, 2014). From a morphological point of view, tree species differ in their foliage distributions and branching patterns under different canopy conditions, resulting in diverge architectures which can be captured by LiDAR. For instance, the foliage of Norway spruce (*Picea abies*) (Fig. 1a) is clustered near the stem with pyramidal crown shape, while the foliage of European beech (*Fagus sylvatica*) (Fig. 1b) is more evenly distributed along the stem and has an oval crown shape. Histograms of laser pulse return frequency within varying height bins illustrate reflection allocation throughout the canopy (Fig. 1). A larger number of returns are reflected within the upper layer of spruce compared to beech. Under leaf-off condition, more returns were allocated towards the bottom of the canopy yet the top of the canopy was still well-represented by the LiDAR point cloud distribution (Fig. 1b). Thus, tree morphology characterized by LiDAR metrics may increase the ability to accurately discriminate tree species.

Over the past decade, a large number of airborne LiDAR-derived metrics have been proposed for tree species classification (Brandtberg, 2007; Brandtberg et al., 2003; Cao et al., 2016; Holmgren and Persson, 2004; Hovi et al., 2016; Kim et al., 2011, 2009; Li et al., 2013; Lin and Herold, 2016; Moffiet et al., 2005; Ørka et al., 2009; Reitberger et al., 2008). Generally, these LiDAR metrics can be categorized into two groups, namely geometric and radiometric metrics. The geometric metrics describe the geometric structure of trees (e.g. crown shape, tree height and crown volume) while the radiometric metrics refer to specific echo parameters that are extracted from the received waveform (e.g. the backscatter cross-section, the energy of laser points, and the distance between two waveform echoes) (Koenig and Höfle, 2016; Wagner, 2010). Particularly, intensity of the backscattered signal is additionally related to foliage type, leaf size, leaf orientation, leaf clumping and foliage density (Kim et al., 2009; Korpela et al., 2010; Suratno et al., 2009). The echo width is dependent on the amount, distribution and orientation of scattering elements along the laser beam direction. These properties can all vary within and between tree species and thus may be useful for differentiating materials and ultimately tree species. Previous studies have demonstrated that LiDAR metrics can be used to improve the mapping accuracy of tree species. However, most of these studies focused on data-driven or algorithm-driven approaches and pursued an optimization of classification accuracy (Fassnacht et al., 2016). Consequently, an in-depth ecological and biological understanding of the linkage between tree species morphology and LiDAR derived metrics has not been performed. Identifying essential LiDAR metrics for tree species classification can not only reduce the "redundant" or "overfitting" caused by highly correlated metrics, but also help us build links between the inherent architectural differences of tree species and how they manifest in LiDAR metrics.

The phenological development of tree species is characterized by distinct seasonal phases of bud burst, leaf flushing, flowering, senescence and dormancy (Calle et al., 2010). The physical changes in canopy structure are particularly prominent for deciduous tree species. The integration of LiDAR data acquired under leaf-on and leaf-off conditions has been proven useful for tree species classification in previous studies (Kim et al., 2009; Ørka et al., 2010; Reitberger et al., 2008; Yao et al., 2012). Although some of these studies suggested several important LiDAR metrics for tree species classification, the majority of them focused on the effects of different canopy conditions on tree properties or only considered a few LiDAR metrics. The role of LiDAR metrics derived from both discrete point and full-waveform data under leaf-on and leaf-off conditions for individual tree species classification has not been explored. Moreover, Sumnall et al. (2016) concluded that the greatest complimentary information about a forest canopy profile can be derived from both leaf-on and leaf-off data rather than discrete return or full-waveform LiDAR data. Nonetheless, due to the incompatibility of LiDAR collections, data availability as well as

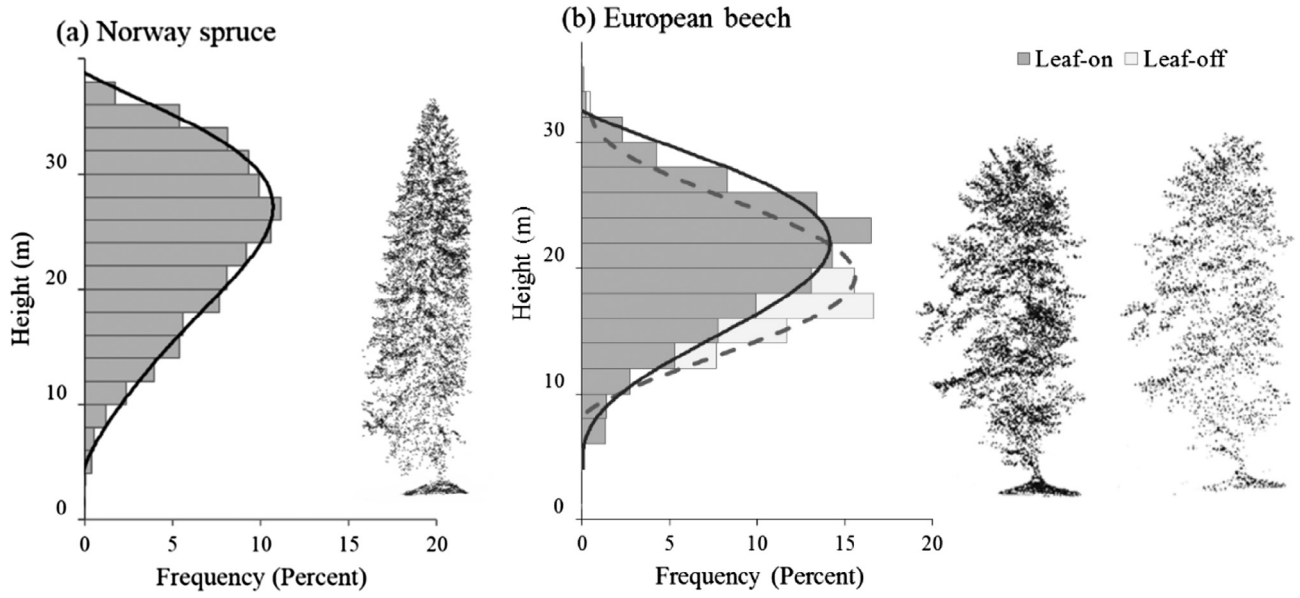

Fig. 1. Example of distributions of canopy laser pulse returns within (a) Norway spruce, and (b) European beech under leaf-on and leaf-off conditions using airborne LiDAR data.

the high costs associated with LiDAR acquisitions and data processing efforts, the full potential of multi-temporal LiDAR datasets for tree species classification has yet to be realized.

This study aims to evaluate the performance of 37 frequently used metrics derived from both discrete return and full-waveform airborne LiDAR data under leaf-on and leaf-off conditions, respectively, for discriminating six different tree species in a mixed temperate forest in Germany. Specifically, we set out to: (1) evaluate the correlation among those commonly used LiDAR metrics, (2) assess the performance of LiDAR metrics for tree species classification under leaf-on and leaf-off conditions and select important input metrics, and (3) identify the most important LiDAR metrics for discriminating tree species and understand how they are linked with tree species morphology.

2. Materials and methods

2.1. Study area and tree species

The study area is located in the Bavarian Forest National Park (49°3′19″N, 13°12′9″E), a mixed temperate forest situated in the south-eastern part of Germany (Fig. 2). The park covers a total area of 24,218 ha with an elevation ranging from approximately 600 m to 1452 m. The forest is dominated by Norway spruce (*Picea abies*), which co-habits with European beech (*Fagus sylvatica*) on the slopes, and silver fir (*Abies alba*) at low and intermediate elevations. Pioneer deciduous species are also present such as white birch (*Betula pendula*), sycamore maple (*Acer pseudoplatanus*), common rowan (*Sorbus aucuparia*), European ash (*Fraxinus excelsior*), European aspen (*Populus tremula*) and Field elm (*Ulmus minor*). However, they only represent 3.3% of the total basal area of the park (Cailleret et al., 2014).

We identified two species-rich sites within the park (Fig. 2) and used them as pilot study areas of interests. Each pilot site is approximately 25 ha (500 m × 500 m). Detailed information about the two study sites, including topographic condition, soil type, tree density, tree height, forest types and stand age classes are provided in Table 1. The spatial location of individual tree species was collected with a Leica Viva GS10 Plus differential GPS (Leica Geosystems AG, Heerbrugg, Switzerland) in July 2016 and July 2017, respectively. The GPS data were post-processed to obtain differentially corrected coordinates with an accuracy less than 0.5 m. In total, we have collected 256 locations of trees at site A and 193 locations of trees at site B.

2.2. Airborne LiDAR data collection and processing

The airborne LiDAR data were acquired on 11 April and 18 August 2016 under leaf-off and leaf-on canopy conditions

Table 1
Characteristics of the two pilot study sites.

	Site A	Site B
Size (ha)	25	25
Elevation (m)	675–732	845–906
Slope (degree)	9.12 ± 5	8.76 ± 3
Soil type	Brown forest soils and peat soils	Loose brown soils and gley soils
Forest type and stand age classes	Mature coniferous and mixed stands	Mature deciduous and mixed stands
Tree density (per ha)	445	458

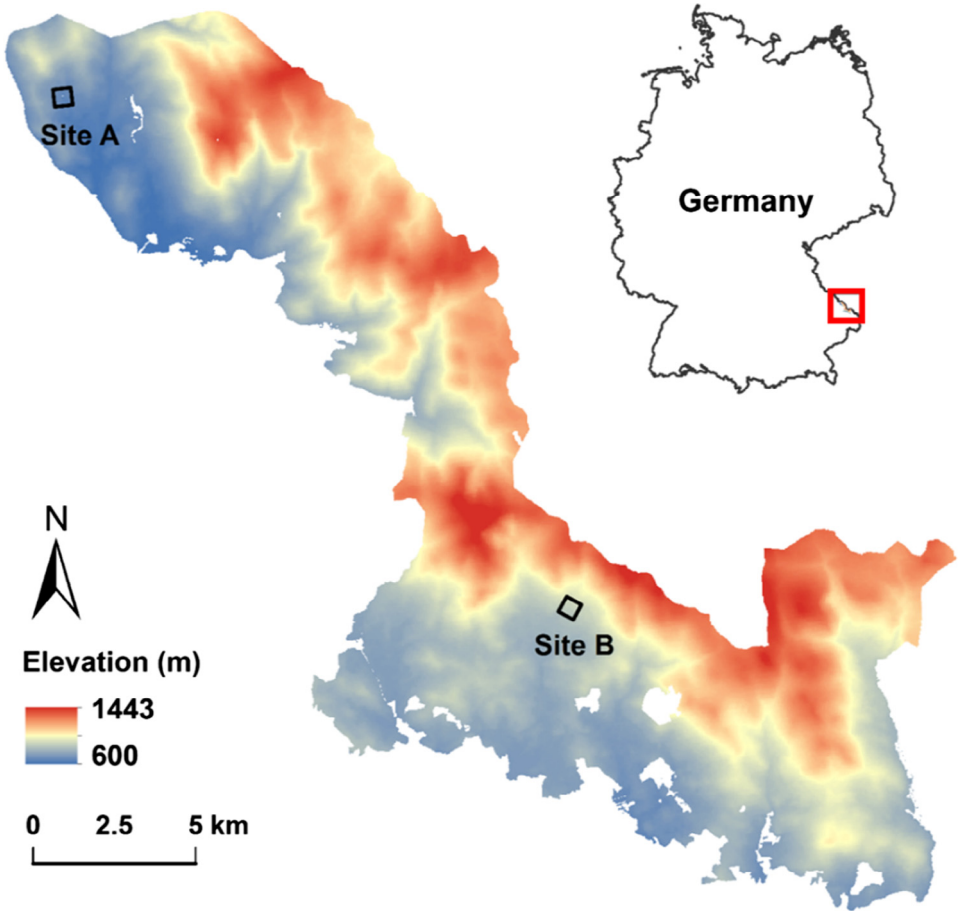

Fig. 2. The study area in Germany and the location of the two pilot study sites in the Bavarian Forest National Park.

respectively, using the Riegl LMS-Q680i scanner (wavelength 1550 nm) integrated in a full-waveform laser scanning system. The two datasets were collected with the same sensor and same settings. The mean flight speed was 50 ms^{-1} and the flying altitude was approximately 300 m above ground. The pulse repetition frequency was 400 kHz with a scan angle around ±15°. The point density was around 70 points/m^2. A total of 21 flight lines were recorded with 50% strip overlap.

Both point cloud data from Gaussian decomposition (Wagner et al., 2006) and raw full-waveform data were delivered by the Milan Flug GmbH Company. The point cloud information contains 3D coordinates (x, y and z), intensity, return number, number of returns, echo width and the GPS timestamp of the return. The extracted point clouds and associated waveforms were stored in the LAS 1.2 format. We used the Lastools software package (LAStools, version 160921, rapidlasso GmbH, http://lastools.org) to create the 0.5 m resolution digital terrain models (DTM) from the LiDAR data. We normalized the height of each LiDAR return to height above ground by subtracting the elevation of the DTM below each point. It should be noted that we have used the same sensor and same settings, calibrating the intensity data of the two LiDAR datasets is not required in this study as suggested by Korpela et al. (2010). In addition, since the altitude of the two LiDAR flights were the same, and our two pilot study sites were topographically similar (having a gentle slope), the intensity normalization for the range between the sensor and object as well as for the incidence angle were therefore ignored (Vain and Kaasalainen, 2011).

2.3. Individual tree segmentation

An adapted 3D segmentation algorithm proposed by Yao et al. (2013) was used to automatically extract individual trees in this study. It is an object-based point cloud analysis approach for tree detection and uses normalized cut segmentation as the core part of the method. The 3D segmentation algorithm is a two-tiered procedure. The steps of the entire procedure are as follows: (i) decomposition of full-waveform data; (ii) local tree maxima filtering; (iii) mean shift clustering; (iv) feature derivation for mean shift clusters; (v) normalized cut segmentation; and (vi) height filtering of the segmentation results. As reported by Yao et al. (2013), with LiDAR data sets at a point density of 25 points/m^2, the experiments using the segmentation algorithm lead to a detection rate of up to 70% for trees in the upper layer, 67% for trees in the middle height layer and 53% for trees in the lower forest layer, which showed 25% improvement compared to that obtained by a former method proposed by Reitberger et al. (2009).

We chose the sample trees and linked them to the correct LiDAR segmentation results for analysis by conducting the following procedures: (1) we first overlaid the location of sample trees with the 3D segmentation results and the aerial photograph (spatial resolution 0.25 m); (2) we then visually verified each sample tree based on the additional information we have recorded in the field (e.g. photos of the sample trees and the species of surrounding trees) as well as the crown shape interpreted from the very high resolution aerial photograph, and tried to connect it with the 3D LiDAR segments; (3) if a sample tree was not detected by the segmentation algorithm, it was removed from further analysis; (4) if a sample tree was assigned to more than one tree position, it was also removed from further analysis. The LiDAR points of each tree segment were extracted and assigned to the corresponding sample trees for both sites A and B. As a result, only 205 sample trees from site A and 158 sample trees from site B were selected and used for the current study. The details of the number and the mean height of each tree species are shown in Table 2.

Table 2
The sample size, mean height and standard deviation (SD) of each tree species in site A and site B.

Tree species	Site A		Site B	
	Sample size	Mean height and SD (m)	Sample size	Mean height and SD (m)
Beech	39	25.9 ± 7.2	29	26.4 ± 5.0
Birch	36	18.2 ± 7.5	29	18.6 ± 4.8
Fir	31	35.7 ± 6.7	21	27.9 ± 7.7
Maple	40	20.7 ± 6.1	37	22.3 ± 7.0
Rowan	21	17.5 ± 6.3	18	16.7 ± 7.2
Spruce	38	28.3 ± 8.0	24	30.7 ± 6.7

2.4. Derivation of LiDAR metrics under leaf-on and leaf-off conditions

The most commonly used tree height related LiDAR metrics are the percentiles of the height distribution of laser pulses classified as canopy hits (Koenig and Höfle, 2016; Li et al., 2013; Lin and Hyyppä, 2016; Ørka et al., 2009; Sumnall et al., 2016; Vauhkonen et al., 2010). The lower limit of the canopy was defined by a threshold value of 2 m. Separate distributions were created for the first and last returns recorded as the percentage of first return to all returns and the percentage of last returns to all returns. From the echo height distribution we computed the maximum, mean, standard deviation, coefficient of variation, kurtosis, skewness, and height percentiles at 5% intervals (Hp5, Hp10, . . ., Hp90, Hp95) of tree height within a tree segment (Andersen et al., 2005; Hopkinson et al., 2006; Lin and Hyyppä, 2016; Muss et al., 2011; Næsset, 2002; Naidoo et al., 2012; Vauhkonen et al., 2010). Due to a strong correlation among the height percentiles metrics between every 5% intervals, we selected the Hp25 and Hp90 percentiles for further analysis. The commonly used tree crown related LiDAR metrics include crown base height, crown volume and crown area which were extracted based on the methods proposed by Yao et al. (2012). The ratio of crown base height to tree height and the ratio of crown volume to crown area were added to reduce the impacts of different tree ages on tree species classification. Moreover, the mean height of first-or-single returns and the mean height of single returns were generated as descriptions to understand how crown shape reflected the different return types of laser pulses. As species identification using 3D features should be based on the architecture of the tree, not on its size, height related LiDAR metrics (i.e. the mean value of height, the standard deviation of height, the height percentiles, the mean height of first-or-single returns and the mean height of single returns) were generated based on normalized heights to eliminate scale dependency. The normalized height is the height of each return above ground divided by the height of the tree it belongs to. In total, 16 geometric metrics were generated as listed in Table 3.

The radiometric metrics used in the tree species classification were derived from the intensity and echo width distributions. In addition to the 25% and 90% percentiles of the intensity, the maximum, mean, standard deviation, coefficient of variation, skewness and kurtosis of intensity within a tree segment were also computed (Dalponte et al., 2008; Heinzel and Koch, 2011; Hovi et al., 2016; Korpela et al., 2010; Lin and Hyyppä, 2016; Ørka et al., 2009; Yao et al., 2012). Similarly, the 25% and 90% percentiles of the echo width, the maximum, mean, standard deviation, coefficient of variation, skewness, and kurtosis of echo width within a tree segment were derived from full-waveform data as the radiometric parameters (Heinzel and Koch, 2011; Höfle et al., 2012; Hovi et al., 2016; Lin, 2015; Yao et al., 2012). Additionally, intensity and echo width with respect to two different echo categories: "first-or-single returns" and "single returns" (i.e. Imean_first and

Table 3
Description of the 37 generated LiDAR metrics.

Metrics	Definition	Metrics	Definition
Geometrics		*Radiometrics*	
Hmax	Maximum height	Imax	Maximum intensity
Hmean	Mean height	Imean	Mean intensity
Hsd	Standard deviation of height	Isd	Standard deviation of intensity
Hcv	Coefficient variation of height	Icv	Coefficient variation of intensity
Hkurt	Kurtosis of height	Ikurt	Kurtosis of intensity
Hskew	Skewness of height	Iskew	Skewness of intensity
Hp25	25th percentile of heights	Ip25	25th percentile of intensity
Hp90	90th percentile of heights	Ip90	90th percentile of intensity
Hmean_first	Mean height of first-or-single returns	Imean_first	Mean intensity of first-or-single returns
Hmean_single	Mean height of single returns	Imean_single	Mean intensity of single returns
First:total_returns	Percentage of first returns above 2 m	Ewmin	Minimum echo width
Last:total_returns	Percentage of last returns above 2 m	Ewmax	Maximum echo width
All_returns	All returns above 2 m	Ewmean	Mean echo width
CBH:H	Ratio of crown base height to height	Ewsd	Standard deviation of echo width
C_volume:area	Ratio of crown volume to crown area	Ewcv	Coefficient variation of echo width
CNR	Canopy relief ratio	Ewkurt	Kurtosis of echo width
		Ewskew	Skewness of echo width
		Ewp25	25th percentile of echo width
		Ewp90	90th percentile of echo width
		Ewmean_first	Mean echo width of first-or-single returns
		Ewmean_single	Mean echo width of single returns

Imean_single for intensity, EWmean_first and EWmean_single for echo width) were also generated from each segment (Hovi et al., 2016; Ørka et al., 2010). In total, 21 radiometric metrics have been generated as listed in Table 3. All metrics were generated under both leaf-on and leaf-off conditions with the R statistical language version 3.3.3 (http://www.r-project.org/).

2.5. Correlation analysis of LiDAR metrics

LiDAR metrics can be useful in species classification if they differ significantly between species (Brandtberg et al., 2003; Holmgren and Persson, 2004). From a statistical point of view, metric selection can reduce the number of input variables which is important for building efficient, stable and transferable classification models. In this study, 37 geometric and radiometric metrics (under both leaf-on and leaf-off conditions) were analysed to reduce the "collinearity" and avoid "overfitting" during the tree species classification process (Table 3). The Pearson's Correlation Coefficient was used to examine the correlations between LiDAR metrics for both the leaf-on and leaf-off datasets. Here, we used the threshold of correlation coefficients between LiDAR metrics of $|r| < 0.70$, as such a threshold has been proved an appropriate indicator for when collinearity begins to severely distort model estimation and subsequent prediction (Dormann et al., 2013).

2.6. Random Forest algorithm

Random Forest is a popular and powerful machine learning algorithm (Belgiu and Drăguţ, 2016; Fassnacht et al., 2016; Ørka et al., 2010; Vauhkonen et al., 2010). We used the Random Forest algorithm, with internal cross-validation, to assess the performance of "selected metrics" for tree species discrimination for leaf-on, leaf-off and combined datasets. During Random Forest classification, approximately one-third of the samples were left out of the input training dataset as "out-of-bag" (OOB) samples to estimate the classification error and derive variable importance (Breiman, 2001). The Mean Decrease Accuracy (MDA) index, which quantifies the degree to which inclusion of a variable in the model decreases the mean squared error, was used to assess the variable importance for classification (Breiman, 2001; Liaw and Wiener, 2002). The mean decrease in accuracy of a variable is determined during the out of bag error calculation phase. The more the accuracy of the random forest decreases due to the exclusion (or permutation) of a single variable, the more important that variable is deemed, and therefore variables with a large mean decrease in accuracy are more important for classification (Teicher et al., 2012). The Random Forest algorithm has several advantages with respect to the current assessment of LiDAR metrics derived from different acquisitions in tree species classification, e.g. (1) it can handle a large number of input variables without variable deletion; (2) it computes an error matrix based on an internal validation process; (3) it estimates which variables are important in the classification, measured as the mean decrease accuracy; (4) the generated forests can be saved for future use on other data; and last but not least (5) it reduces overfitting and is therefore more accurate than equivalent discriminative, or boosted regression based methods trained on the same data (Cootes et al., 2012). However, similar to most classifiers, Random Forest algorithm can also suffer from the curse of learning from an extremely imbalanced training dataset (Chen et al., 2004). Hence, we used the Random Forest algorithm to derive both classification accuracy as well as the variable importance in this study. The classification was carried out with the R package "*randomForest*" (Liaw and Wiener, 2002). We tested different values for the Random Forest parameter "Ntree" (i.e. number of trees grown) and parameter "Mtry" (i.e. number of predictors sampled for splitting at each node), varying in each test from 1 to 500 and from 1 to 30, respectively, and we set up a loop to run the Random Forest algorithm for each combination of parameters and chose the model with the best classification performance. Then we applied this model in study site B for classification, accuracy assessment and metrics evaluation using samples independent of the samples used to develop the model in study site A, and assessed the robustness and transferability of "selected metrics" by comparing the importance of selected metrics.

2.7. Classification accuracy assessment

We used producer's accuracy, user's accuracy, overall accuracy and kappa coefficient to assess the classification results (Cohen, 1960). We also used the McNemar's test to determine whether statistically significant differences exist between classifications (de Leeuw et al., 2006; McNemar, 1947).

Using Random Forest we iterated with the 12 metrics generated during the first step of metrics selection under leaf-on and leaf-off conditions using 205 sample trees in study site A. The performance of the LiDAR metrics was further verified by 158 independent sample trees collected in study site B by using the Random Forest model established in study site A. The classification results and metrics importance derived from site B were compared to the results of site A under all leaf-on, leaf-off and integration conditions.

2.8. Determining the importance of the LiDAR metrics

We calculated classification accuracy and evaluated metrics importance under leaf-on and leaf-off conditions. For each condition, we chose the 7 top-ranked metrics (14 metrics in total) as the input of final classification. We selected 14 metrics because inclusion of more features did not increase the classification accuracy significantly, which was also demonstrated by Li et al. (2013). After selection of important LiDAR metrics under leaf-on and leaf-off conditions, we input the 14 top-ranked metrics as the integration metrics of leaf-on and leaf-off conditions for the tree species classification. We applied the classification model with the same parameter settings to study site B, and recorded the performance of classification and the importance of input metrics. Then we identified the most consistently significant metrics and evaluated the contribution of each metric based on the classification results.

3. Results

3.1. Correlation of LiDAR metrics

High correlation ($|r| > 0.7$) was observed among many of the geometric and radiometric metrics derived from both leaf-on and leaf-off conditions (Fig. 3). For the geometric metrics, high correlation was found between the height related metrics such as Hmax, Hmean, Hsd, Hcv, Hskew, Hp25, Hp90, Hmean_first, Hmean_single and CNR. For radiometric metrics, the echo width related metrics presented stronger correlations between the metrics in comparison to intensity related metrics. Specifically, three echo width related metrics, i.e. Ewmean, Ewsd and Ewcv were highly correlated to each other under both leaf-on and leaf-off conditions. As a result, only 30 out of 74 LiDAR metrics (combining both leaf-on and leaf-off conditions) were found with an absolute correlation coefficients less than 0.70.

3.2. LiDAR metrics selection

Firstly, we evaluated 37 LiDAR metrics (under both leaf-on and leaf-off condition) based on correlation coefficients as well as the ranking of their importance using the Mean Decrease Accuracy index (MDA). We retained the metrics with a correlation coefficient $|r| < 0.70$ and the higher ranked metric when two compared metrics had $|r| > 0.70$. Then, we used 12 top-ranked significant metrics as

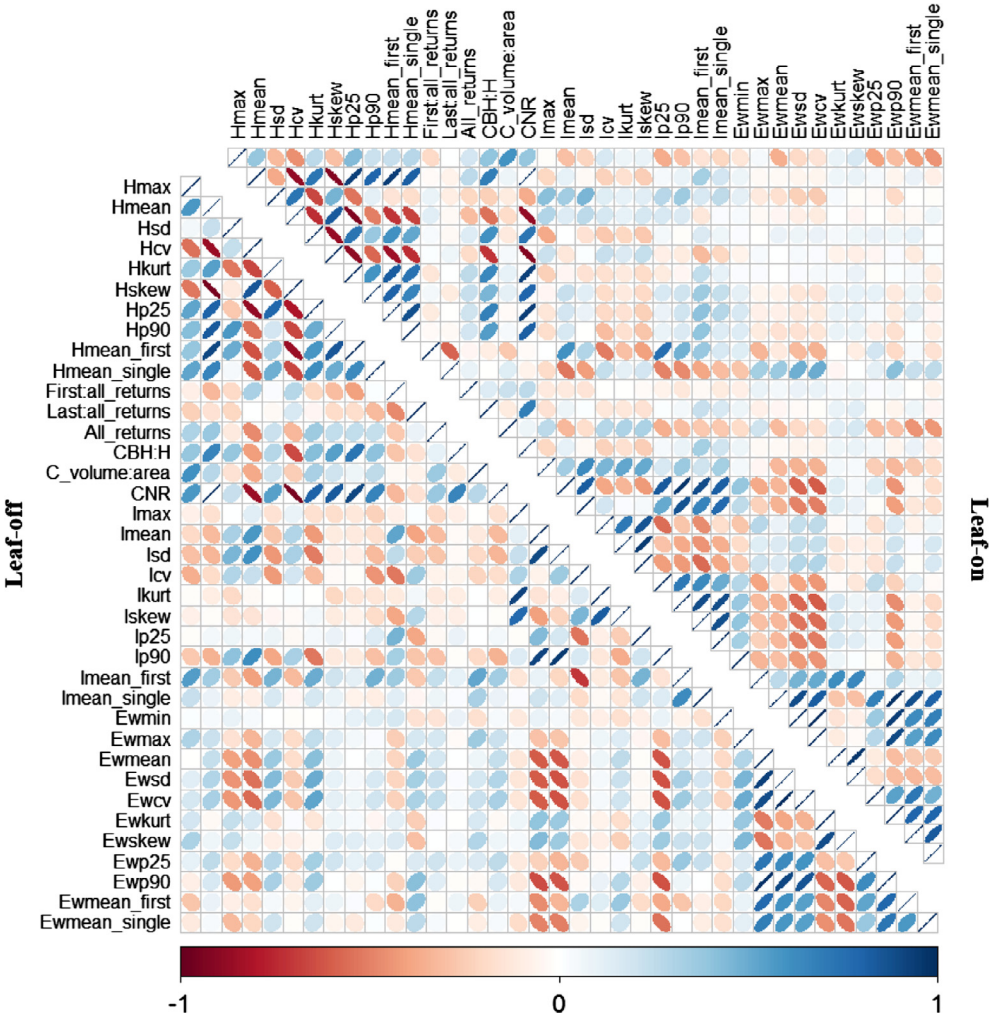

Fig. 3. Cross-correlation matrix of the 37 LiDAR metrics derived under leaf-off (lower) and leaf-on (upper) conditions. Blue colours indicate positive correlations and red colours indicate negative correlations. See Table 3 for definitions of the metrics.

the input for further classification (Table 4). Finally, we selected the top 7 metrics from each condition (i.e. leaf-on and leaf-off) as the final input metrics for classification based on MDA (Table 4).

3.3. Comparison of classification accuracies

The classification results produced by the Random Forest algorithm are presented in Table 5. It is shown that there was no statistically significant difference in tree species mapping accuracy between the use of leaf-on and leaf-off LiDAR metrics (McNemar's test, $p > 0.05$) (Table 6). However, combining leaf-on and leaf-off LiDAR metrics significantly increased the overall accuracy from 58.2% (leaf-on) and 62.0% (leaf-off) to 66.5% as well as the kappa coefficient from 0.47 (leaf-on) and 0.51 (leaf-off) to 0.58 (McNemar's test, $p < 0.05$) (Table 6).

We executed the selected LiDAR metrics in study site B in order to assess the robustness and transferability of the selected metrics. The difference in the classification performance was minor between leaf-on and leaf-off conditions, while combining LiDAR metrics derived under leaf-on and leaf-off conditions significantly improved the accuracy (Table 6). Both the classification in site A and site B generated modest and comparable classification accuracy. For individual tree species, beech, birch and spruce were classified with higher user's and producer's accuracy under leaf-off rather than leaf-on condition (Table 5). Rowan was misclassified under leaf-on and leaf-off conditions using selected metrics, and only a slight improvement occurred using the combined leaf-on and leaf-off datasets.

3.4. Performance of LiDAR metrics in tree species classification

Fig. 4 presents the relative importance and ranking of the selected LiDAR metrics for tree species classification for the two pilot study sites based on leaf-on, leaf-off and their combination. It indicates that the significant metrics and their ranks vary under different conditions. However, Imean_first appeared as the first-ranked metrics under every condition in both sites A and B. When metrics selected from leaf-on and leaf-off datasets were combined, 4 out of 5 top ranked metrics were the same as those derived in site A (Fig. 4c and f), which were all radiometric metrics. Hmean_single had a performance comparable to the Imean_first under leaf-off and combination conditions in site A, however, it did not show superior performance in the classification of site B. Comparing important metrics under each condition, Imean_first and EWmean consistently appeared as top 5 metrics through different canopy conditions.

We also tested the accumulated contribution rate increased through increasing the number of selected metrics for classification. Adding LiDAR metrics produced the largest increase in the classification contribution rate, from 65% to 100%, reached the first peak (96.2%) using the top 5 metrics, and stabilizing around 93% at 10 metrics, which supporting the choice of 10 features as a reasonable limit for species classification. The first 5 metrics were selected as the best performed for the separation of the tree species

Table 6
McNemar's test for pairwise comparison between classification results derived from the three datasets (leaf-on, leaf-off, and integration). The number in the table is p value. The number with an asterisk (*) indicates that the difference between classifications is significant at a 5% significant level.

	Site A		Site B	
	Leaf-off	Integration	Leaf-off	Integration
Leaf-on	0.16	<0.01*	0.11	<0.01*
Leaf-off		0.09		0.02*

Table 4
Selected LiDAR metrics derived under leaf-on and leaf-off conditions and their Mean Decrease Accuracy (MDA). The top 7 metrics indicated by the asterisk (*) from each condition (i.e. leaf-on and leaf-off) were used as final input metrics for tree species classification.

Leaf-on	MDA	Leaf-off	MDA	Leaf-on and leaf-off	MDA
*Imean_first	14.221	*Imean_first	13.185	Imean_first_off	13.01
*Ewmean	12.185	*Hmean_single	11.796	Hmean_single_off	12.64
*Hmax	11.530	*Ewmean	10.471	Imean_first_on	11.15
*Imean_single	9.117	*Icv	10.313	Icv_off	10.64
*Imean	8.551	*Ewmean_first	10.024	Ewmean_on	10.11
*Hmean_single	8.386	*Hmean_first	9.256	Hmax_on	10.09
*Ewmean_first	8.071	*Hmean	9.021	Ewmean_off	9.83
Ewmean_single	7.623	Hcv	8.309	Ewmean_first_on	9.15
Hmean_first	7.220	Ewp90	8.249	Ewmean_first_off	9.13
Ip90	6.844	Hp25	7.881	Hmean_single_on	8.95
Hp90	3.698	Ewmean_single	6.822	Imean_on	8.92
C_volume:area	1.172	Hkurt	5.587	Hmean_first_off	8.13
				Imean_single_on	7.11
				Hmean_off	5.88

Table 5
Comparison of overall accuracy and kappa coefficient for tree species classification using leaf-on, leaf-off and combination of leaf-on and leaf-off LiDAR metrics.

Tree species	Site A						Site B					
	Leaf-on		Leaf-off		Integration		Leaf-on		Leaf-off		Integration	
	UA (%)	PA (%)	UA (%)	PA (%)	UA (%)	PA (%)	UA (%)	PA (%)	UA (%)	PA (%)	UA (%)	PA (%)
Beech	54.1	57.1	67.6	67.6	64.9	64.9	48.3	50.0	58.6	28.6	55.2	55.2
Birch	54.5	50.0	57.6	57.6	63.6	58.3	75.9	73.3	79.3	76.7	82.8	82.8
Maple	68.9	60.8	66.7	63.3	64.4	65.9	67.6	61.0	70.3	61.9	78.4	65.9
Rowan	26.3	38.5	21.5	40.0	36.8	63.6	31.3	16.7	27.8	50.0	33.3	46.2
Fir	66.7	57.1	66.7	60.6	73.3	68.8	52.4	61.1	61.9	56.5	57.1	70.6
Spruce	56.1	65.7	61.0	56.8	65.9	60.0	58.3	58.3	70.8	68.0	75.0	69.2
OA	57.1%		60.0%		62.4%		58.2%		62.0%		66.5%	
Kappa	0.46		0.49		0.54		0.47		0.51		0.58	

OA: overall accuracy; UA: user's accuracy; PA: producer's accuracy.

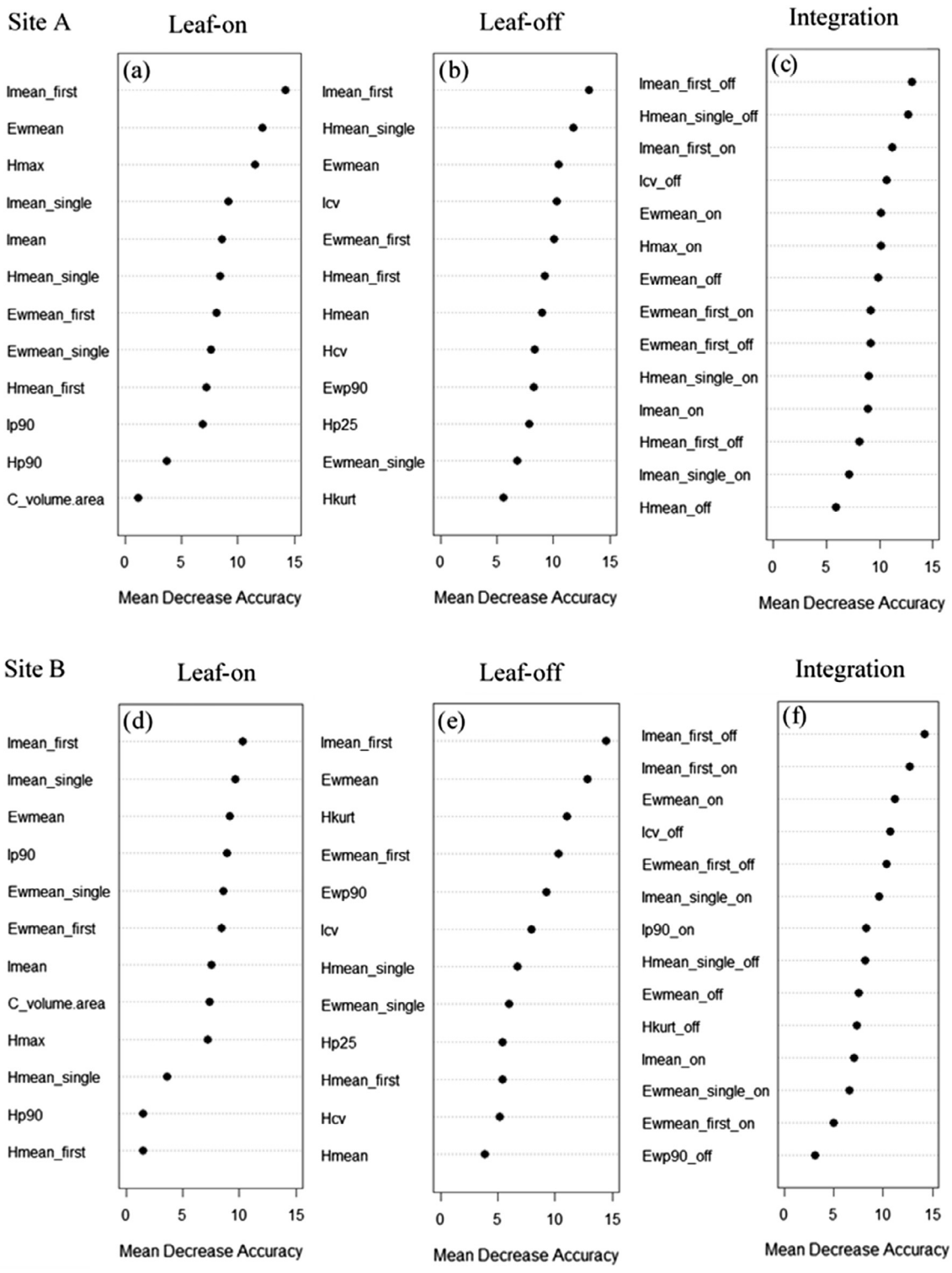

Fig. 4. The relative importance and ranking of the selected LiDAR metrics for tree species classification under different conditions derived from the pilot study site A and site B. The Mean Decreasing Accuracy indicates importance by how much the permutation (effective elimination) of a given variable decreases the accuracy of the overall fit. Metrics that are associated with the greatest decrease in accuracy coefficient following permutation are the most important.

of interest according to the MDA in Random Forest that globally maximize the fitness function through iterations.

3.5. The capability of metrics for tree species discrimination

The differences between the six tree species for the top 4 ranked metrics are plotted in Fig. 5. It can be observed that the ability of the 4 most important metrics for tree species discrimination varies for each species under different conditions. It is evident that coniferous trees have a higher value of mean intensity of first returns compared to deciduous trees under leaf-off condition, while the difference of this metric between coniferous trees and deciduous trees becomes smaller under leaf-on condition (Fig. 5a). A similar pattern can be observed in Fig. 5d about the normalized mean

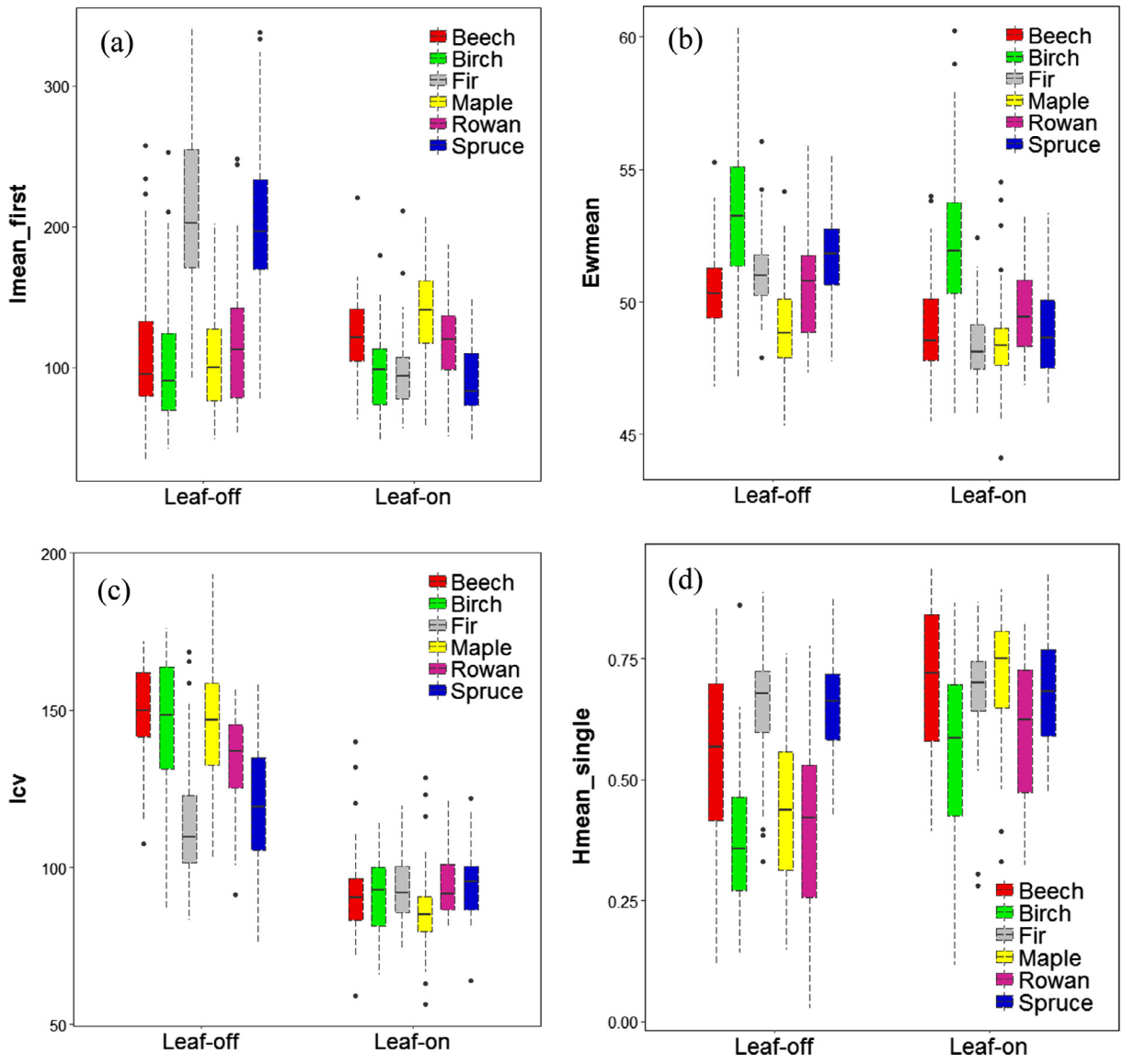

Fig. 5. Box plots of mean intensity of first-or-single returns (a), mean value of echo width (b), coefficient variation of intensity (c), and normalized mean height of single returns (d) among six tree species under leaf-on and leaf-off conditions. The value of each metrics is based on the sample trees from both site A and site B.

height of single returns. Fig. 5c shows a distinct difference of coefficient variation of intensity between leaf-on and leaf-off conditions among 6 species, which differentiates coniferous trees from deciduous trees under leaf-off condition. Similarly, the mean value of echo width shows a superior ability to separate birch from other 5 tree species, especially under leaf-on condition (Fig. 5b).

4. Discussion and conclusions

In this study, we generated a set of geometric and radiometric metrics from airborne LiDAR data under leaf-on and leaf-off conditions and evaluated their performance for individual tree species discrimination in a mixed temperate forest in Germany. Our results demonstrated that radiometric features consistently contributed a higher accuracy compared to geometric features for classifying tree species under both leaf-on and leaf-off conditions. Specifically, the mean intensity of first-or-single returns as well as the mean value of echo width were identified as the most robust LiDAR metrics for discriminating six typical tree species in Central Europe. The importance of features derived from the first and the last returns for tree species classification was reported by Ørka et al. (2010) and the current study specified and verified this result. We found that the mean intensity of first-or-single returns was least sensitive to the canopy condition and well represented the structural and morphological characteristics of trees, which contributed most to the accuracy of tree species classification. Both the mean intensity of first-or-single returns and echo width are metrics which contain radiometric and geometric (3D) information. The mean intensity of first-or-single returns is derived from the outer "crown shell", which means narrow and peaked branch tips result in an increased proportion of partial hits by footprint (Korpela et al., 2013). It also implies that the difference in the spatial distribution of branches between different species is most prominent at the top of canopy. The major structural differences among species that are reflected in LiDAR metrics generally occur at the top crown layers rather than middle and low stem layers, which explained why radiometric metrics played an important role in species discrimination in comparison geometric metrics. However, the value of the mean intensity of first-or-single returns of deciduous trees in

our study did not show a significant difference between leaf-off and leaf-on conditions (Fig. 5a) – this may be due to an earlier spring leaf unfolding phenology that occurred in 2016 in our study area. Contradictory to the study conducted by Sumnall et al. (2016), where echo width metrics were considered relatively unimportant for forest inventory purposes, we found that the mean echo width within a tree segment led to more stable performance than geometric features, with an important contribution from the intensity metrics (Fig. 4). It should be noted that echo width metrics did not show considerable superiorities compared to height related metrics under leaf-off condition. The plausible explanation for this is that the difference of echo width metrics between coniferous species and deciduous species becomes narrower due to leaf loss of deciduous trees and the exposure of their branches, which, at the same time, can be well represented by geometric features. Those results indicated radiometric features have greater potential for representing species-specific characteristic, which is supported by previous studies (Heinzel and Koch, 2011; Hovi et al., 2016; Kim et al., 2009; Ørka et al., 2009, 2010; Sumnall et al., 2016). By contrast, many geometric features are affected by tree height, which may be also related to other properties, such as crown volume, crown shape and the interior structure of the tree crown. Misclassifications may be due to the similarities of the morphology among different tree species and also the architectural variations within the same tree species. The cause of structural deviations including tree competition as well as differences in environmental niche (such as temperature or soil condition) may also alter the shapes of tree crowns, which introduces further uncertainties in the classification. Therefore, discriminating tree species based on LiDAR derived geometric features may be challenging in complex natural forests, while using radiometric metrics provides better classification performance by their species-specific characters.

Several studies have discussed the influence of canopy conditions on tree properties from airborne LiDAR data (Kim, 2007; Kim et al., 2009; Naesset, 2005; Ørka et al., 2010). Our results showed that there was a slight improvement of classification accuracy when using leaf-off acquisition compared to leaf-on acquisition, which also has been supported by Reitberger et al. (2008) and Heurich (2006) in the same study area. However, there was no statistically significant difference in tree species mapping accuracy between the use of leaf-on and leaf-off LiDAR metrics (Table 6). We also found that a large proportion of important metrics were generated under leaf-off condition. It may be because the metrics derived under leaf-off condition offer a higher potential for representing the inner architecture of crowns, which give radiometric features a better chance to describe the interior structure of trees. Combining leaf-on and leaf-off datasets resulted in higher separability between tree species than using LiDAR data from one season. Notably, there was always a significant improvement in classification performance when combining leaf-on and leaf-off datasets compared to leaf-on dataset (Table 6). This result indicated that individual tree species discrimination could benefit more from the leaf-off acquisitions by obtaining more accurate species-specific LiDAR metrics. We gained an overall accuracy (OA) (66.5%) and kappa value (0.58) for all six species when combining leaf-on and leaf-off datasets in site B, which is slightly lower than many previous studies. However, we found a reasonable degree of accuracy by using solely airborne LiDAR data for individual tree species mapping in a natural mixed forest.

Ørka et al. (2010) indicated that there may be a set of features that can be applicable in tree species classification across different acquisitions. In this study, we tested and verified the robustness and transferability of important LiDAR metrics, which serve as the substantial markers of tree species that can be used for further study. It should be noted that our analysis was based on two study sites with relatively low variability regarding forest type and topography. Therefore, the applicability of the important metrics needs to be further tested in other study sites. Moreover, the point density of LiDAR data in this study is higher than in many other studies and the effect of point density on feature derivation and the classification still needs to be evaluated. Previous studies also indicated that high point density (i.e. >40 points/m^2) airborne LiDAR data can be used to extract more detailed structural features such as internal foliage and branch patterns of an individual tree, which may further the distinction between different tree species (Li et al., 2013; Vauhkonen et al., 2014). Obtaining larger sample trees and improving individual tree segmentation accuracy may also lead to higher classification accuracy and better understanding of LiDAR metrics performance during classification. Building links between the inherent architectural differences of tree species and how they manifest in LiDAR metrics remains a critical endeavour for remote sensing researchers. As a result, gathering field measurements and discovering relationships between crown structural characteristics and waveform metrics remains important to improve the physical interpretability of the airborne LiDAR metrics, with some of the relationships found here, serving as a ground for potential further investigations.

Acknowledgements

The first author is financially supported by the China Scholarship Council under Grant 201506650001, co-funded by the ITC Research Fund. We are grateful to Prof. Dr. Peter Krzystek from Munich University of Applied Sciences for performing the tree segmentation. We also acknowledge the support of the "Data Pool Forestry" data-sharing initiative of the Bavarian Forest National Park. We would like to thank all the anonymous reviewers and the associate editor (Prof. Dr. Sanna Kaasalainen) for their constructive comments and suggestions on this manuscript.

References

Alonzo, M., Bookhagen, B., Roberts, D.A., 2014. Urban tree species mapping using hyperspectral and lidar data fusion. Remote Sens. Environ. 148, 70–83.
Andersen, H.-E., McGaughey, R.J., Reutebuch, S.E., 2005. Estimating forest canopy fuel parameters using LIDAR data. Remote Sens. Environ. 94, 441–449.
Asner, G.P., Knapp, D.E., Kennedy-Bowdoin, T., Jones, M.O., Martin, R.E., Boardman, J., Hughes, R.F., 2008. Invasive species detection in Hawaiian rainforests using airborne imaging spectroscopy and LiDAR. Remote Sens. Environ. 112, 1942–1955.
Aspinall, R.J., 2002. Use of logistic regression for validation of maps of the spatial distribution of vegetation species derived from high spatial resolution hyperspectral remotely sensed data. Ecol. Model. 157, 301–312.
Baldeck, C.A., Asner, G.P., Martin, R.E., Anderson, C.B., Knapp, D.E., Kellner, J.R., Wright, S.J., 2015. Operational tree species mapping in a diverse tropical forest with airborne imaging spectroscopy. PLoS ONE 10, e0118403.
Belgiu, M., Drăguţ, L., 2016. Random forest in remote sensing: a review of applications and future directions. ISPRS J. Photogramm. Remote Sens. 114, 24–31.
Boschetti, M., Boschetti, L., Oliveri, S., Casati, L., Canova, I., 2007. Tree species mapping with Airborne hyper-spectral MIVIS data: the Ticino Park study case. Int. J. Remote Sens. 28, 1251–1261.
Brandtberg, T., 2007. Classifying individual tree species under leaf-off and leaf-on conditions using airborne lidar. ISPRS J. Photogramm. Remote Sens. 61, 325–340.
Brandtberg, T., Warner, T.A., Landenberger, R.E., McGraw, J.B., 2003. Detection and analysis of individual leaf-off tree crowns in small footprint, high sampling density lidar data from the eastern deciduous forest in North America. Remote Sens. Environ. 85, 290–303.
Breiman, L., 2001. Random forests. Mach. Learn. 45, 5–32.
Cailleret, M., Heurich, M., Bugmann, H., 2014. Reduction in browsing intensity may not compensate climate change effects on tree species composition in the Bavarian Forest National Park. For. Ecol. Manage. 328, 179–192.
Calle, Z., Schlumpberger, B.O., Piedrahita, L., Leftin, A., Hammer, S.A., Tye, A., Borchert, R., 2010. Seasonal variation in daily insolation induces synchronous bud break and flowering in the tropics. Trees 24, 865–877.
Cao, L., Coops, N.C., Innes, J.L., Dai, J., Ruan, H., She, G., 2016. Tree species classification in subtropical forests using small-footprint full-waveform LiDAR data. Int. J. Appl. Earth Obs. Geoinf. 49, 39–51.

Chen, C., Liaw, A., Breiman, L., 2004. Using Random Forest to Learn Imbalanced Data. University of California, Berkeley, p. 110.
Clark, M.L., Clark, D.B., Roberts, D.A., 2004. Small-footprint lidar estimation of sub-canopy elevation and tree height in a tropical rain forest landscape. Remote Sens. Environ. 91, 68–89.
Cohen, J., 1960. A coefficient of agreement for nominal scales. Educ. Psychol. Measur. 20, 37–46.
Coops, N.C., Hilker, T., Wulder, M.A., St-Onge, B., Newnham, G., Siggins, A., Trofymow, J.T., 2007. Estimating canopy structure of Douglas-fir forest stands from discrete-return LiDAR. Trees 21, 295–310.
Cootes, T.F., Ionita, M.C., Lindner, C., Sauer, P., 2012. Robust and accurate shape model fitting using random forest regression voting. In: Fitzgibbon, A., Lazebnik, S., Perona, P., Sato, Y., Schmid, C. (Eds.), Computer Vision – ECCV 2012: 12th European Conference on Computer Vision, Florence, Italy, October 7-13, 2012, Proceedings, Part VII. Springer Berlin Heidelberg, Berlin, Heidelberg, pp. 278–291.
Dalponte, M., Bruzzone, L., Gianelle, D., 2008. Fusion of hyperspectral and LIDAR remote sensing data for classification of complex forest areas. IEEE Trans. Geosci. Remote Sens. 46, 1416–1427.
Dalponte, M., Ørka, H.O., Ene, L.T., Gobakken, T., Næsset, E., 2014. Tree crown delineation and tree species classification in boreal forests using hyperspectral and ALS data. Remote Sens. Environ. 140, 306–317.
de Leeuw, J., Jia, H., Yang, L., Liu, X., Schmidt, K., Skidmore, A.K., 2006. Comparing accuracy assessments to infer superiority of image classification methods. Int. J. Remote Sens. 27, 223–232.
Dormann, C.F., Elith, J., Bacher, S., Buchmann, C., Carl, G., Carré, G., Marquéz, J.R.G., Gruber, B., Lafourcade, B., Leitão, P.J., Münkemüller, T., McClean, C., Osborne, P. E., Reineking, B., Schröder, B., Skidmore, A.K., Zurell, D., Lautenbach, S., 2013. Collinearity: a review of methods to deal with it and a simulation study evaluating their performance. Ecography 36, 27–46.
Fassnacht, F.E., Latifi, H., Stereńczak, K., Modzelewska, A., Lefsky, M., Waser, L.T., Straub, C., Ghosh, A., 2016. Review of studies on tree species classification from remotely sensed data. Remote Sens. Environ. 186, 64–87.
Feret, J.-B., Asner, G.P., 2013. Tree species discrimination in tropical forests using airborne imaging spectroscopy. IEEE Trans. Geosci. Remote Sens. 51, 73–84.
Ghiyamat, A., Shafri, H.Z.M., 2010. A review on hyperspectral remote sensing for homogeneous and heterogeneous forest biodiversity assessment. Int. J. Remote Sens. 31, 1837–1856.
Heinzel, J., Koch, B., 2011. Exploring full-waveform LiDAR parameters for tree species classification. Int. J. Appl. Earth Obs. Geoinf. 13, 152–160.
Heinzel, J., Koch, B., 2012. Investigating multiple data sources for tree species classification in temperate forest and use for single tree delineation. Int. J. Appl. Earth Obs. Geoinf. 18, 101–110.
Heurich, M., 2006. Evaluierung und entwicklung von automatiserten erfassung von waldstructuren aus daten flugzuggetragener fernerkundungssenoren. Forstkuche Forshungsberichte München, 2002, p. 329.
Höfle, B., Hollaus, M., Hagenauer, J., 2012. Urban vegetation detection using radiometrically calibrated small-footprint full-waveform airborne LiDAR data. ISPRS J. Photogramm. Remote Sens. 67, 134–147.
Holmgren, J., Persson, Å., 2004. Identifying species of individual trees using airborne laser scanner. Remote Sens. Environ. 90, 415–423.
Hopkinson, C., Chasmer, L., Lim, K., Treitz, P., Creed, I., 2006. Towards a universal lidar canopy height indicator. Can. J. Rem. Sens. 32, 139–152.
Hovi, A., Korhonen, L., Vauhkonen, J., Korpela, I., 2016. LiDAR waveform features for tree species classification and their sensitivity to tree- and acquisition related parameters. Remote Sens. Environ. 173, 224–237.
Hyyppä, J., Kelle, O., Lehikoinen, M., Inkinen, M., 2001. A segmentation-based method to retrieve stem volume estimates from 3-D tree height models produced by laser scanners. IEEE Trans. Geosci. Remote Sens. 39, 969–975.
Immitzer, M., Atzberger, C., Koukal, T., 2012. Tree species classification with random forest using very high spatial resolution 8-band worldview-2 satellite data. Remote Sens. 4, 2661–2693.
Jones, T.G., Coops, N.C., Sharma, T., 2010. Assessing the utility of airborne hyperspectral and LiDAR data for species distribution mapping in the coastal Pacific Northwest, Canada. Remote Sens. Environ. 114, 2841–2852.
Kim, S., 2007. Individual Tree Species Identification Using LIDAR-Derived Crown Structures and Intensity Data. University of Washington.
Kim, S., Hinckley, T., Briggs, D., 2011. Classifying individual tree genera using stepwise cluster analysis based on height and intensity metrics derived from airborne laser scanner data. Remote Sens. Environ. 115, 3329–3342.
Kim, S., McGaughey, R.J., Andersen, H.E., Schreuder, G., 2009. Tree species differentiation using intensity data derived from leaf-on and leaf-off airborne laser scanner data. Remote Sens. Environ. 113, 1575–1586.
Koenig, K., Höfle, B., 2016. Full-waveform airborne laser scanning in vegetation studies—a review of point cloud and waveform features for tree species classification. Forests 7, 198.
Korpela, I., Hovi, A., Korhonen, L., 2013. Backscattering of individual LiDAR pulses from forest canopies explained by photogrammetrically derived vegetation structure. ISPRS J. Photogramm. Remote Sens. 83, 81–93.
Korpela, I., Ørka, H.O., Maltamo, M., Tokola, T., Hyyppä, J., 2010. Tree species classification using airborne LiDAR–effects of stand and tree parameters, downsizing of training set, intensity normalization, and sensor type. Silva Fennica 44, 319–339.
Leckie, D.G., Gougeon, F.A., Walsworth, N., Paradine, D., 2003. Stand delineation and composition estimation using semi-automated individual tree crown analysis. Remote Sens. Environ. 85, 355–369.
Leckie, D.G., Tinis, S., Nelson, T., Burnett, C., Gougeon, F.A., Cloney, E., Paradine, D., 2005. Issues in species classification of trees in old growth conifer stands. Can. J. Remote Sens. 31, 175–190.
Li, J., Hu, B., Noland, T.L., 2013. Classification of tree species based on structural features derived from high density LiDAR data. Agric. For. Meteorol. 171–172, 104–114.
Liaw, A., Wiener, M., 2002. Classification and regression by randomForest. R News 2, 18–22.
Lin, Y.-C., 2015. Normalization of echo features derived from full-waveform airborne laser scanning data. Remote Sens. 7, 2731–2751.
Lin, Y., Herold, M., 2016. Tree species classification based on explicit tree structure feature parameters derived from static terrestrial laser scanning data. Agric. For. Meteorol. 216, 105–114.
Lin, Y., Hyyppä, J., 2016. A comprehensive but efficient framework of proposing and validating feature parameters from airborne LiDAR data for tree species classification. Int. J. Appl. Earth Obs. Geoinf. 46, 45–55.
Lindberg, E., Eysn, L., Hollaus, M., Holmgren, J., Pfeifer, N., 2014. Delineation of tree crowns and tree species classification from full-waveform airborne laser scanning data using 3-D ellipsoidal clustering. IEEE J. Sel. Top. Appl. Earth Obs. Remote Sens. 7, 3174–3181.
McNemar, Q., 1947. Note on the sampling error of the difference between correlated proportions or percentages. Psychometrika 12, 153–157.
Moffiet, T., Mengersen, K., Witte, C., King, R., Denham, R., 2005. Airborne laser scanning: exploratory data analysis indicates potential variables for classification of individual trees or forest stands according to species. ISPRS J. Photogramm. Remote Sens. 59, 289–309.
Muss, J.D., Mladenoff, D.J., Townsend, P.A., 2011. A pseudo-waveform technique to assess forest structure using discrete lidar data. Remote Sens. Environ. 115, 824–835.
Næsset, E., 2002. Predicting forest stand characteristics with airborne scanning laser using a practical two-stage procedure and field data. Remote Sens. Environ. 80, 88–99.
Naesset, E., 2005. Assessing sensor effects and effects of leaf-off and leaf-on canopy conditions on biophysical stand properties derived from small-footprint airborne laser data. Remote Sens. Environ. 98, 356–370.
Naidoo, L., Cho, M.A., Mathieu, R., Asner, G., 2012. Classification of savanna tree species, in the Greater Kruger National Park region, by integrating hyperspectral and LiDAR data in a Random Forest data mining environment. ISPRS J. Photogramm. Remote Sens. 69, 167–179.
Onojeghuo, A.O., Blackburn, G.A., 2011. Optimising the use of hyperspectral and LiDAR data for mapping reedbed habitats. Remote Sens. Environ. 115, 2025–2034.
Ørka, H.O., Næsset, E., Bollandsås, O.M., 2009. Classifying species of individual trees by intensity and structure features derived from airborne laser scanner data. Remote Sens. Environ. 113, 1163–1174.
Ørka, H.O., Næsset, E., Bollandsås, O.M., 2010. Effects of different sensors and leaf-on and leaf-off canopy conditions on echo distributions and individual tree properties derived from airborne laser scanning. Remote Sens. Environ. 114, 1445–1461.
Pcorona, A.B., Corona, P., Marchetti, M., 2006. European Forest Types Categories and Types for Sustainable Forest Management Reporting and Policy.
Reitberger, J., Krzystek, P., Stilla, U., 2008. Analysis of full waveform LIDAR data for the classification of deciduous and coniferous trees. Int. J. Remote Sens. 29, 1407–1431.
Reitberger, J., Schnorr, C., Krzystek, P., Stilla, U., 2009. 3D segmentation of single trees exploiting full waveform LIDAR data. ISPRS J. Photogramm. Remote Sens. 64, 561–574.
Shang, X., Chazette, P., 2014. Interest of a full-waveform flown UV lidar to derive forest vertical structures and aboveground carbon. Forests 5, 1454–1480.
Skidmore, A.K., Pettorelli, N., Coops, N.C., Geller, G.N., Hansen, M., Lucas, R., Mücher, C.A., O'Connor, B., Paganini, M., Pereira, H.M., 2015. Environmental science: agree on biodiversity metrics to track from space. Nature 523, 403–405.
Somers, B., Asner, G.P., 2014. Tree species mapping in tropical forests using multi-temporal imaging spectroscopy: wavelength adaptive spectral mixture analysis. Int. J. Appl. Earth Obs. Geoinf. 31, 57–66.
Sumnall, M.J., Hill, R.A., Hinsley, S.A., 2016. Comparison of small-footprint discrete return and full waveform airborne lidar data for estimating multiple forest variables. Remote Sens. Environ. 173, 214–223.
Suratman, M.N., 2012. Tree Species Diversity and Forest Stand Structure of Pahang National Park, Malaysia. INTECH Open Access Publisher.
Suratno, A., Seielstad, C., Queen, L., 2009. Tree species identification in mixed coniferous forest using airborne laser scanning. ISPRS J. Photogramm. Remote Sens. 64, 683–693.
Teicher, M.H., Polcari, A., Fourligas, N., Vitaliano, G., Navalta, C.P., 2012. Hyperactivity persists in male and female adults with ADHD and remains a highly discriminative feature of the disorder: a case-control study. BMC Psych. 12, 190.
Vain, A., Kaasalainen, S., 2011. Correcting Airborne Laser Scanning Intensity Data. Laser Scanning, Theory and Applications. InTech.
Vauhkonen, J., Korpela, I., Maltamo, M., Tokola, T., 2010. Imputation of single-tree attributes using airborne laser scanning-based height, intensity, and alpha shape metrics. Remote Sens. Environ. 114, 1263–1276.
Vauhkonen, J., Ørka, H.O., Holmgren, J., Dalponte, M., Heinzel, J., Koch, B. (2014). Tree species recognition based on airborne laser scanning and complementary data sources. In: Forestry Applications of Airborne Laser Scanning. Springer, pp. 135–156.

Wagner, W., 2010. Radiometric calibration of small-footprint full-waveform airborne laser scanner measurements: basic physical concepts. ISPRS J. Photogramm. Remote Sens. 65, 505–513.

Wagner, W., Ullrich, A., Ducic, V., Melzer, T., Studnicka, N., 2006. Gaussian decomposition and calibration of a novel small-footprint full-waveform digitising airborne laser scanner. ISPRS J. Photogramm. Remote Sens. 60, 100–112.

Yao, W., Krzystek, P., Heurich, M., 2012. Tree species classification and estimation of stem volume and DBH based on single tree extraction by exploiting airborne full-waveform LiDAR data. Remote Sens. Environ. 123, 368–380.

Yao, W., Krzystek, P., Heurich, M., 2013. Enhanced detection of 3D individual trees in forested areas using airborne full-waveform LiDAR data by combining normalized cuts with spatial density clustering. ISPRS Ann. Photogram., Rem. Sens. Spatial Inf. Sci. 1, 349–354.